Universität Karlsruhe (TH)
Institut für Baustatik

A new stabilized one–point integrated shear–elastic plate element

W. Wagner, F. Gruttmann

Mitteilung 5(2004)

Universität Karlsruhe (TH)
Institut für Baustatik

A new stabilized one–point integrated shear–elastic plate element

W. Wagner, F. Gruttmann

Mitteilung 5(2004)

© Prof. Dr.–Ing. W. Wagner
Institut für Baustatik
Universität Karlsruhe
Postfach 6980
76128 Karlsruhe

Telefon: (0721) 608–2280
Telefax: (0721) 608–6015
E–mail: bs@.uni-karlsruhe.de
Internet: http://www.bs.uni-karlsruhe.de

European Congress on Computational Methods in Applied Sciences and Engineering
ECCOMAS 2004
P. Neittaanmäki, T. Rossi, K. Majava, and O. Pironneau (eds.)
R. Owen and M. Mikkola (assoc. eds.)
Jyväskylä, 24–28 July 2004

A NEW STABILIZED ONE–POINT INTEGRATED SHEAR–ELASTIC PLATE ELEMENT

Friedrich Gruttmann[⋆], Werner Wagner[†]

[⋆] Institut für Werkstoffe und Mechanik im Bauwesen
Alexanderstr. 7, D-64283 Technical University of Darmstadt, Germany
e-mail: gruttmann@iwmb.tu-darmstadt.de, web page: http://www.iwmb.tu-darmstadt.de

[†] Institut für Baustatik
Kaiserstr. 12, D-76131 University of Karlsruhe(TH), Germany
e-mail: ww@bs.uni-karlsruhe.de, web page: http://www.bs.uni-karlsruhe.de

Key words: Hellinger–Reissner variational principle, Mindlin–Reissner plate theory, quadrilateral element, effective one point integration and stabilization matrix, bending patch test.

Abstract. *A new and efficient formulation for a quadrilateral Mindlin–Reissner plate element is presented. A Hellinger–Reissner functional with independent displacements, rotations and stress resultants is used in case of a linear isotropic elastic material. Within the mixed formulation the stress resultants are interpolated using five parameters for the bending moments and four parameters for the shear forces. The hybrid element stiffness matrix resulting from the stationary condition can be integrated analytically and thus is obtained by a one point integration and a stabilization matrix. The element possesses a correct rank, does not show shear locking and is applicable for the evaluation of displacements and stress resultants within the whole range of thin and thick plates.*

1 INTRODUCTION

In the past, considerable research efforts have been directed towards the development of efficient and reliable finite plate elements and numerous publications can be found in the literature see e.g. the textbook [1].

Here we mention among may others the so–called DKT and DKQ elements, where the Kirchhoff constraints are only fulfilled at discrete points of a thin plate, see e.g. [2]. Most of the work has been focussed on the Mindlin–Reissner model, e.g. [3,4], which by–passes the difficulties caused by C^1–requirements of the classical Kirchhoff theory, e.g. [1,5]. However for the standard bilinear interpolation for the transverse displacements and rotations severe shear locking occur for thin plates. A simple method to avoid this locking behavior is the application of reduced or selective reduced integration, see e.g. [6,7], which leads then to a rank deficiency of the element stiffness matrix. Hence several authors have developed stabilization techniques to regain the correct rank, e.g. [8,9]. These techniques have been extended and refined for different boundary value problems in [10], where stabilization matrices on basis of the enhanced strain method have been derived. A further method uses substitute shear strain fields [11], subsequently extended and reformulated in [12,13] and [14–16]. For mixed hybrid models the choice of assumed internal stress fields is particularly crucial, e.g. [17].

The paper is organized as follows. The variational formulation for a linear plate accounting for transverse shear strains is based on a Hellinger–Reissner functional. The interpolation functions for the displacements, strains and stress resultants are specified and explicit expressions for the element matrices are derived. The analytical integration leads to the element stiffness matrix which is obtained by one-point integration and a stabilization matrix. Several examples demonstrate the efficiency of the developed finite plate element.

2 BASIC EQUATIONS

2.1 Variational Formulation

For a the description of a plate we introduce the domain Ω, the boundary Γ, the thickness h, a transverse load $\bar{\mathbf{p}} = [p, 0, 0]^T$ in Ω and boundary loads $\bar{\mathbf{t}} = [\bar{p}, \bar{m}_x, \bar{m}_y]^T$ on Γ_σ. The variational formulation is based on a Hellinger–Reissner functional.

$$\Pi_{HR}(\mathbf{u}, \boldsymbol{\sigma}) = \int_{(\Omega)} (\boldsymbol{\varepsilon}^T \boldsymbol{\sigma} - \frac{1}{2} \boldsymbol{\sigma}^T \mathbf{C}^{-1} \boldsymbol{\sigma})\, dA - \int_{(\Omega)} \mathbf{u}^T \bar{\mathbf{p}}\, dA - \int_{(\Gamma_\sigma)} \mathbf{u}^T \bar{\mathbf{t}}\, ds \quad \rightarrow \quad \text{stat.} \qquad (1)$$

Here, the displacement field is $\mathbf{u} = [w, \beta_x, \beta_y]^T$, with the transverse deflection w and the rotations β_x and β_y , see Fig. 1. Furthermore, we introduce the vector of stress resultants $\boldsymbol{\sigma} = [m_x, m_y, m_{xy}, q_x, q_y]^T$ with the bending moments m_x, m_y, m_{xy} and the shear forces

q_x, q_y. Within a Mindlin–Reissner theory the strains read

$$\boldsymbol{\varepsilon} = \begin{bmatrix} \kappa_x \\ \kappa_y \\ 2\kappa_{xy} \\ \gamma_x \\ \gamma_y \end{bmatrix} = \begin{bmatrix} \beta_{x,x} \\ \beta_{y,y} \\ \beta_{x,y} + \beta_{y,x} \\ \beta_x + w_{,x} \\ \beta_y + w_{,y} \end{bmatrix} . \tag{2}$$

Furthermore, the constitutive matrix for linear isotropic elasticity is introduced as

$$\mathbf{C} = \begin{bmatrix} \mathbf{C}^b & \mathbf{0} \\ \mathbf{0} & \mathbf{C}^s \end{bmatrix} , \quad \mathbf{C}^b = D \begin{bmatrix} 1 & \nu & 0 \\ \nu & 1 & 0 \\ 0 & 0 & \dfrac{1-\nu}{2} \end{bmatrix} , \quad \mathbf{C}^s = \kappa\, G\, h \begin{bmatrix} 1 & 0 \\ 0 & 1 \end{bmatrix} \tag{3}$$

with the bending rigidity $D = \frac{Eh^3}{12\,(1-\nu^2)}$, Young´s modulus E, shear modulus G, Poisson´s ratio ν and shear correction factor $\kappa = \frac{5}{6}$. The stationary condition yields

$$\delta\Pi_{HR}(\mathbf{u}, \boldsymbol{\sigma}, \delta\mathbf{u}, \delta\boldsymbol{\sigma}) = \int_{(\Omega)} [\delta\boldsymbol{\varepsilon}^T\, \boldsymbol{\sigma} + \delta\boldsymbol{\sigma}^T\, (\boldsymbol{\varepsilon} - \mathbf{C}^{-1}\boldsymbol{\sigma}) - \delta\mathbf{u}^T \bar{\mathbf{p}}]\, dA - \int_{(\Gamma_\sigma)} \delta\mathbf{u}^T\, \bar{\mathbf{t}}\, ds = 0 \tag{4}$$

with virtual displacements and stresses $\delta\mathbf{u} = [\delta w, \delta\beta_x, \delta\beta_y]^T$, $\delta\boldsymbol{\sigma} = [\delta m_x, \delta m_y, \delta m_{xy}, \delta q_x, \delta q_y]^T$.

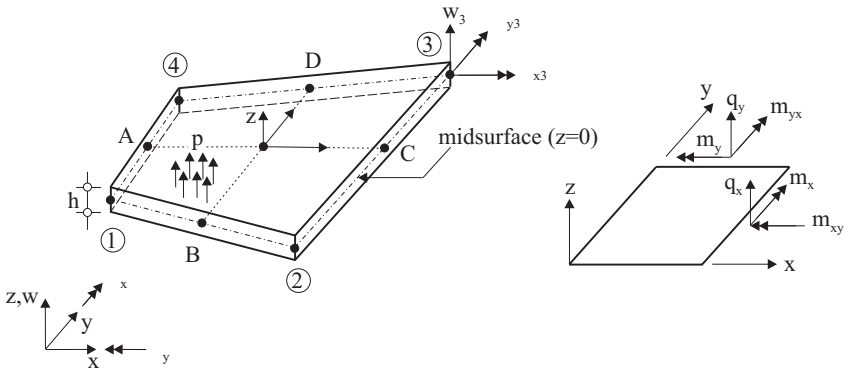

Figure 1: Quadrilateral plate element

2.2 Finite Element Equations

For a quadrilateral element we exploit the isoparametric concept with coordinates ξ, η defined in the unit square $\{\xi, \eta\} \in [-1, 1]$, see Fig. 1, and interpolate the transverse displacements and rotations as well as the virtual quantities using bilinear functions

$$w = \mathbf{N}^T \mathbf{w}\,, \quad \beta_x = \mathbf{N}^T \boldsymbol{\beta}_x\,, \quad \beta_y = \mathbf{N}^T \boldsymbol{\beta}_y\,. \tag{5}$$

Here, $\mathbf{w}$, $\boldsymbol{\beta}_x$, $\boldsymbol{\beta}_y$ denote the nodal displacements and rotations and $\mathbf{N}$ the vector of the bilinear shape functions with

$$\begin{aligned} \mathbf{N} &= [N_1, N_2, N_3, N_4]^T = \mathbf{a}_0 + \xi\,\mathbf{a}_1 + \eta\,\mathbf{a}_2 + \xi\eta\,\mathbf{h} \\ \mathbf{a}_0 &= \frac{1}{4}\begin{bmatrix} 1 \\ 1 \\ 1 \\ 1 \end{bmatrix} \qquad \mathbf{a}_1 = \frac{1}{4}\begin{bmatrix} -1 \\ 1 \\ 1 \\ -1 \end{bmatrix} \qquad \mathbf{a}_2 = \frac{1}{4}\begin{bmatrix} -1 \\ -1 \\ 1 \\ 1 \end{bmatrix} \qquad \mathbf{h} = \frac{1}{4}\begin{bmatrix} 1 \\ -1 \\ 1 \\ -1 \end{bmatrix} \end{aligned} \tag{6}$$

In order to fulfill the bending patch test, see e.g. Taylor et al. [18], we approximate the shear strains with independent interpolation functions proposed in [14] as follows

$$\begin{bmatrix} \gamma_x \\ \gamma_y \end{bmatrix} = \mathbf{J}^{-1} \begin{bmatrix} \gamma_\xi \\ \gamma_\eta \end{bmatrix} \quad \text{where} \quad \begin{aligned} \gamma_\xi &= \frac{1}{2}[(1-\eta)\gamma_\xi^B + (1+\eta)\gamma_\xi^D] \\ \gamma_\eta &= \frac{1}{2}[(1-\xi)\gamma_\eta^A + (1+\xi)\gamma_\eta^C] \end{aligned} \tag{7}$$

with the Jacobian matrix computed with the nodal coordinates $\mathbf{x} = [x_1, x_2, x_3, x_4]^T$ and $\mathbf{y} = [y_1, y_2, y_3, y_4]^T$

$$\mathbf{J} = \begin{bmatrix} x_{,\xi} & y_{,\xi} \\ x_{,\eta} & y_{,\eta} \end{bmatrix} = \begin{bmatrix} \mathbf{x}^T(\mathbf{a}_1 + \eta\mathbf{h}) & \mathbf{y}^T(\mathbf{a}_1 + \eta\mathbf{h}) \\ \mathbf{x}^T(\mathbf{a}_2 + \xi\mathbf{h}) & \mathbf{y}^T(\mathbf{a}_2 + \xi\mathbf{h}) \end{bmatrix}. \tag{8}$$

Thus, with eq. (7) the covariant components of the shear strains are transformed to the cartesian coordinate system. The determinant of $\mathbf{J}$ yields

$$\det \mathbf{J} = j_0 + \xi\, j_1 + \eta\, j_2 \quad \text{with} \quad \begin{aligned} j_0 &= (\mathbf{x}^T\mathbf{a}_1)(\mathbf{y}^T\mathbf{a}_2) - (\mathbf{x}^T\mathbf{a}_2)(\mathbf{y}^T\mathbf{a}_1) \\ j_1 &= (\mathbf{x}^T\mathbf{a}_1)(\mathbf{y}^T\mathbf{h}) - (\mathbf{y}^T\mathbf{a}_1)(\mathbf{x}^T\mathbf{h}) \\ j_2 &= (\mathbf{y}^T\mathbf{a}_2)(\mathbf{x}^T\mathbf{h}) - (\mathbf{x}^T\mathbf{a}_2)(\mathbf{y}^T\mathbf{h})\,. \end{aligned} \tag{9}$$

The strains at the midside nodes A, B, C, D, see Fig. 1, are specified as follows

$$\begin{aligned} \gamma_\xi^M &= [x_{,\xi}\,\beta_x + y_{,\xi}\,\beta_y + w_{,\xi}\,]^M \qquad M = B, D \\ \gamma_\eta^L &= [x_{,\eta}\,\beta_x + y_{,\eta}\,\beta_y + w_{,\eta}\,]^L \qquad L = A, C \end{aligned} \tag{10}$$

where the following quantities are given with the bilinear interpolation (5)

$$\begin{aligned} \beta_\alpha^A &= \tfrac{1}{2}(\beta_{\alpha 4} + \beta_{\alpha 1})\,, \quad \alpha = x, y & w_{,\eta}^A &= \tfrac{1}{2}(w_4 - w_1) \\ \beta_\alpha^B &= \tfrac{1}{2}(\beta_{\alpha 1} + \beta_{\alpha 2}) & w_{,\xi}^B &= \tfrac{1}{2}(w_2 - w_1) \\ \beta_\alpha^C &= \tfrac{1}{2}(\beta_{\alpha 2} + \beta_{\alpha 3}) & w_{,\eta}^C &= \tfrac{1}{2}(w_3 - w_2) \\ \beta_\alpha^D &= \tfrac{1}{2}(\beta_{\alpha 3} + \beta_{\alpha 4}) & w_{,\xi}^D &= \tfrac{1}{2}(w_3 - w_4) \\ \mathbf{r}_{,\eta}^A &= \tfrac{1}{2}(\mathbf{r}_4 - \mathbf{r}_1)\,, \quad \mathbf{r} = \begin{bmatrix} x \\ y \end{bmatrix} & \mathbf{r}_{,\eta}^C &= \tfrac{1}{2}(\mathbf{r}_3 - \mathbf{r}_2) \\ \mathbf{r}_{,\xi}^B &= \tfrac{1}{2}(\mathbf{r}_2 - \mathbf{r}_1) & \mathbf{r}_{,\xi}^D &= \tfrac{1}{2}(\mathbf{r}_3 - \mathbf{r}_4) \end{aligned} \tag{11}$$

Considering (2) and (5) - (11) the approximation of the strains is now obtained by

$$\boldsymbol{\varepsilon}^h = \mathbf{B}\,\mathbf{v}\,, \quad \mathbf{B} = [\mathbf{B}_1, \mathbf{B}_2, \mathbf{B}_3, \mathbf{B}_4]\,, \quad \mathbf{v} = [\mathbf{v}_1, \mathbf{v}_2, \mathbf{v}_3, \mathbf{v}_4]^T\,, \tag{12}$$

where $\mathbf{v}_I = [w_I, \beta_{xI}, \beta_{yI}]^T$ and the submatrices for bending and shear are

$$\mathbf{B}_I = \begin{bmatrix} \mathbf{B}_I^b \\ \mathbf{B}_I^s \end{bmatrix}\,,\; \mathbf{B}_I^b = \begin{bmatrix} 0 & N_{I,x} & 0 \\ 0 & 0 & N_{I,y} \\ 0 & N_{I,y} & N_{I,x} \end{bmatrix}\,,\; \mathbf{B}_I^s = \mathbf{J}^{-1} \begin{bmatrix} N_{I,\xi} & b_I^{11} N_{I,\xi} & b_I^{12} N_{I,\xi} \\ N_{I,\eta} & b_I^{21} N_{I,\eta} & b_I^{22} N_{I,\eta} \end{bmatrix} \tag{13}$$

with

$$\begin{aligned} b_I^{11} &= \xi_I\, x^M_{,\xi} & b_I^{12} &= \xi_I\, y^M_{,\xi} \\ b_I^{21} &= \eta_I\, x^L_{,\eta} & b_I^{22} &= \eta_I\, y^L_{,\eta}\,. \end{aligned} \tag{14}$$

The coordinates of the unit square are $\xi_I \in \{-1, 1, 1, -1\}$, $\eta_I \in \{-1, -1, 1, 1\}$ and the allocation of the midside nodes to the corner nodes is given by $(I, M, L) \in \{(1, B, A); (2, B, C); (3, D, C); (4, D, A)\}$.

The stress field $\boldsymbol{\sigma}$ is interpolated as follows

$$\begin{aligned} \boldsymbol{\sigma}^h &= \mathbf{S}\,\boldsymbol{\beta} \qquad \mathbf{S} = [\mathbf{1}_{(5\times5)}, \tilde{\mathbf{S}}] \qquad \boldsymbol{\beta} = \left[\boldsymbol{\beta}^0, \boldsymbol{\beta}^1\right]^T \\ \tilde{\mathbf{S}} &= \begin{bmatrix} J_{11}^0 J_{11}^0 (\eta - \bar\eta) & J_{21}^0 J_{21}^0 (\xi - \bar\xi) & 0 & 0 \\ J_{12}^0 J_{12}^0 (\eta - \bar\eta) & J_{22}^0 J_{22}^0 (\xi - \bar\xi) & 0 & 0 \\ J_{11}^0 J_{12}^0 (\eta - \bar\eta) & J_{21}^0 J_{22}^0 (\xi - \bar\xi) & 0 & 0 \\ 0 & 0 & J_{11}^0 (\eta - \bar\eta) & J_{21}^0 (\xi - \bar\xi) \\ 0 & 0 & J_{12}^0 (\eta - \bar\eta) & J_{22}^0 (\xi - \bar\xi) \end{bmatrix}\,, \end{aligned} \tag{15}$$

where the vectors $\boldsymbol{\beta}^0$ and $\boldsymbol{\beta}^1$ contain 5 and 4 parameters, respectively. The transformation coefficients $J_{\alpha\beta}^0$ in (15) denote the components of the Jacobian matrix (8) evaluated at the element center ($\xi = 0, \eta = 0$) and transform the contravariant components of the stress resultant tensors to the cartesian basis system. The coefficients have to be constant in order to fulfill the patch test. The constants $\bar\xi$ and $\bar\eta$ which are introduced to obtain decoupled matrices denote the coordinates of the center of gravity of the element

$$\bar\xi = \frac{1}{A_e} \int\limits_{(\Omega_e)} \xi\, dA = \frac{1}{3}\frac{j_1}{j_0} \qquad \bar\eta = \frac{1}{A_e} \int\limits_{(\Omega_e)} \eta\, dA = \frac{1}{3}\frac{j_2}{j_0}\,. \tag{16}$$

The element area is given by $A_e = 4 j_0$.

Inserting (12) and (15) and the corresponding equations for the virtual stresses and virtual strains into the stationary condition (4) yields

$$\delta\Pi_{HR}^h = \sum_{e=1}^{numel} \begin{bmatrix} \delta\boldsymbol{\beta} \\ \delta\mathbf{v} \end{bmatrix}_e^T \left\{ \begin{bmatrix} -\mathbf{H} & \mathbf{G} \\ \mathbf{G}^T & \mathbf{0} \end{bmatrix} \begin{bmatrix} \boldsymbol{\beta} \\ \mathbf{v} \end{bmatrix} - \begin{bmatrix} \mathbf{0} \\ \mathbf{f} \end{bmatrix} \right\}_e = 0\,, \tag{17}$$

where *numel* denotes the total number of plate elements to discretize the problem and the virtual element vectors $\delta\boldsymbol{\beta}$ and $\delta\mathbf{v}$, respectively. The element load vector $\mathbf{f} = [\mathbf{f}_1, \mathbf{f}_2, \mathbf{f}_3, \mathbf{f}_4]^T$ which follows from the external virtual work is identical with a pure displacement formulation. For a constant load p one obtains $\mathbf{f}_I = [f_I^w, 0, 0]^T$ with

$$f_I^w = A_e\, p\, (a_{0I} + \frac{1}{3}\frac{j_1}{j_0} a_{1I} + \frac{1}{3}\frac{j_2}{j_0} a_{2I})\,, \tag{18}$$

where a_{0I}, a_{1I}, a_{2I} are the components of the vectors defined in (6).

Furthermore the matrices $\mathbf{H}$ and $\mathbf{G}$ are introduced

$$\mathbf{H} := \int\limits_{(\Omega_e)} \mathbf{S}^T \mathbf{C}^{-1} \mathbf{S}\, dA\,, \qquad \mathbf{G} := \int\limits_{(\Omega_e)} \mathbf{S}^T \mathbf{B}\, dA\,. \tag{19}$$

Since all integrants in (19) involve only polynomials of the coordinates ξ and η the integration for the element matrices can be carried out analytically. The components of the matrix $\mathbf{H}$ are given by

$$\mathbf{H} = \begin{bmatrix} A_e\, \mathbf{C}^{-1} & \mathbf{0} \\ \mathbf{0} & \mathbf{h} \end{bmatrix} \qquad \text{with} \qquad \mathbf{h} = \begin{bmatrix} \mathbf{h}^b & \mathbf{0} \\ \mathbf{0} & \mathbf{h}^s \end{bmatrix}_{(4\times 4)} \tag{20}$$

and

$$\begin{aligned}
h^b_{11} &= \frac{4A_e f_{11}}{Eh^3}\,(J^{02}_{11} + J^{02}_{12})^2 \qquad & h^b_{22} &= \frac{4A_e f_{22}}{Eh^3}\,(J^{02}_{21} + J^{02}_{22})^2 \\
h^b_{12} &= h^b_{21} = \frac{4A_e f_{12}}{Eh^3}\,\left[(J^0_{11}\,J^0_{21} + J^0_{22}J^0_{12})^2 - \nu\,(J^0_{11}\,J^0_{22} - J^0_{12}J^0_{21})^2\right] \\
h^s_{11} &= \frac{A_e f_{11}}{3\kappa G h}\,(J^{02}_{11} + J^{02}_{12}) \qquad & h^s_{22} &= \frac{A_e f_{22}}{3\kappa G h}\,(J^{02}_{21} + J^{02}_{22}) \\
h^s_{12} &= h^s_{21} = \frac{A_e f_{12}}{3\kappa G h}\,(J^0_{11}\,J^0_{21} + J^0_{22}J^0_{12})
\end{aligned} \tag{21}$$

$$f_{11} = 1 - \frac{1}{3}\left(\frac{j_2}{j_0}\right)^2 \qquad f_{22} = 1 - \frac{1}{3}\left(\frac{j_1}{j_0}\right)^2 \qquad f_{12} = -\frac{1}{3}\frac{j_1}{j_0}\frac{j_2}{j_0}\,.$$

Furthermore the matrix $\mathbf{G}$ is obtained by analytical integration as follows

$$\mathbf{G} = [\mathbf{G}_1, \mathbf{G}_2, \mathbf{G}_3, \mathbf{G}_4] \qquad \mathbf{G}_I = \begin{bmatrix} A_e\, \mathbf{B}^0_I \\ \mathbf{g}_I \end{bmatrix} \qquad \mathbf{g}_I = \frac{1}{3} A_e \gamma_I \begin{bmatrix} 0 & J^0_{11} & J^0_{12} \\ 0 & J^0_{21} & J^0_{22} \\ 1 & \gamma^{11}_I & \gamma^{12}_I \\ 1 & \gamma^{21}_I & \gamma^{22}_I \end{bmatrix} \tag{22}$$

with $\mathbf{B}_I^0 = \mathbf{B}_I(\xi = 0, \eta = 0)$ and

$$\begin{aligned}
\gamma_I &= h_I - \frac{j_2}{j_0} a_{1I} - \frac{j_1}{j_0} a_{2I} \\
\gamma_I^{11} &= (b_I^{11} h_I - b_I^{11} \frac{j_2}{j_0} a_{1I} - b_I^{21} \frac{j_1}{j_0} a_{2I})/\gamma_I \\
\gamma_I^{12} &= (b_I^{12} h_I - b_I^{12} \frac{j_2}{j_0} a_{1I} - b_I^{22} \frac{j_1}{j_0} a_{2I})/\gamma_I \\
\gamma_I^{21} &= (b_I^{21} h_I - b_I^{11} \frac{j_2}{j_0} a_{1I} - b_I^{21} \frac{j_1}{j_0} a_{2I})/\gamma_I \\
\gamma_I^{22} &= (b_I^{22} h_I - b_I^{12} \frac{j_2}{j_0} a_{1I} - b_I^{22} \frac{j_1}{j_0} a_{2I})/\gamma_I \,.
\end{aligned} \tag{23}$$

The parameters h_I, a_{1I}, a_{2I} are the components of the nodal vectors defined in (6), whereas the $b_I^{\alpha\beta}$ are defined in (14). Since the interpolation of the stress resultants are discontinuous at the element boundaries, the stress parameters are eliminated on element level

$$\boldsymbol{\beta} = \mathbf{H}^{-1} \mathbf{G}\, \mathbf{v} \,. \tag{24}$$

Thus considering (20) and (22) one obtains the element stiffness matrix

$$\begin{aligned}
\mathbf{k}^e = \mathbf{G}^T \mathbf{H}^{-1} \mathbf{G} &= \mathbf{k}_0 + \mathbf{k}_{stab} \\
\mathbf{k}_{IK} &= A_e \mathbf{B}_I^{0T} \mathbf{C} \mathbf{B}_K^0 + \mathbf{g}_I^T \mathbf{h}^{-1} \mathbf{g}_K \,.
\end{aligned} \tag{25}$$

Here, $\mathbf{k}_0$ denotes the stiffness of a one–point integrated Mindlin–Reissner plate element with substitute shear strains and $\mathbf{k}_{stab}$ the stabilization matrix. The matrix $\mathbf{h}$ according to (20) consists of two submatrices of order two and thus can easily be inverted. The element possesses with three zero eigenvalues the correct rank.

3 EXAMPLES

The derived element formulation has been implemented in an extended version of the general purpose finite element program FEAP, see Zienkiewicz and Taylor [1].

3.1 Constant bending patch test

First we investigate the element behaviour within a constant bending patch test as is depicted in Fig. 2. A rectangular plate of length a and width b supported at three corners is loaded by a concentrated load at the fourth corner and by bending moments at the corners. The geometrical and material data and the loading parameters are given. The solution of the problem can be computed analytically. The vertical displacement of node 1 is $w_1 = 12.48$ and the bending moments $m_x = m_y = m_{xy} = 1.0$ are constant throughout the plate.

The present element fulfills the patch test as Fig. 3 shows.

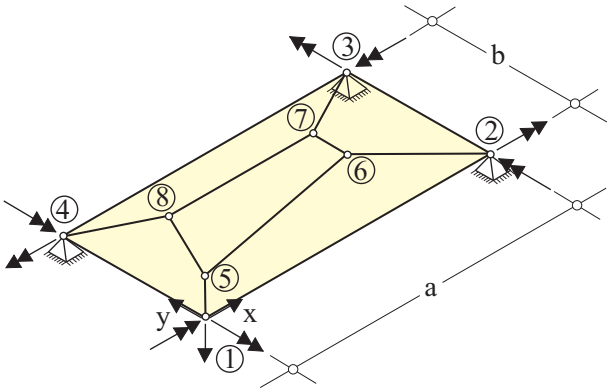

Node	F_z	$\bar{m}_x$	$\bar{m}_y$
1	-2	20	-10
2	0	20	10
3	0	-20	10
4	0	-20	-10

$a = 40 \quad E = 10^6$
$b = 20 \quad \nu = 0.3$
$h = 0.1$

Figure 2: Rectangular plate, patch of 5 elements

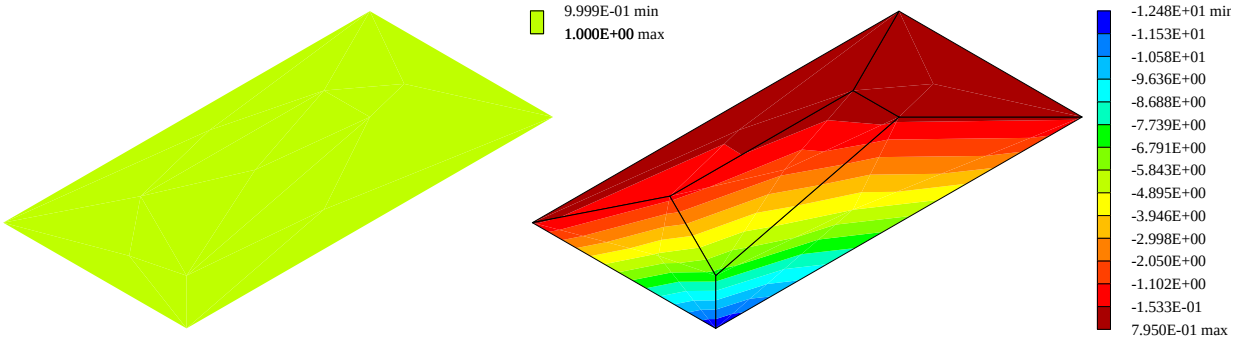

Figure 3: Bending moment m_x and displacement w for the present element

3.2 Clamped square plate subjected to a concentrated load

The problem with geometrical and material data is defined in Fig. 4. The mesh consists of 2×2 elements over a quarter of the plate, where fourfold symmetry has been used. Here the influence of element distorsion is tested, where one inner node is moved by $0 < s < 10$ in x- and y-direction. An analytical Kirchhoff solution for the center deflection yields $w = 0.0056\ Fa^2/D = 1$, see e.g. [5]. The sensitivity of different element formulations with respect to the distorsion parameter s is depicted in Fig. 5. The DKQ–element [2] behaves relatively insensitive with respect to the mesh distorsion and yields for the present coarse mesh a solution which is too weak. The results computed with the new element are slightly better than with the Bathe/Dvorkin element [15]. The clamped plate allows a calculation without stabilization matrix, since the hourglass modes are suppressed by the boundary conditions. Thus for the present example the best results are obtained with an one point integrated element U_1. However this is not the case for arbitrary boundary conditions. Results for the Belytschko/Tsay [8] element are similar to the element U_1 in the recommended range for the stabilization parameter $0.02 \leq r_w \leq 0.05$. A contour plot of w with a distorsion parameter $s = 10$ is given in Fig. 5 for the present element.

$$
\begin{aligned}
a &= 100 \\
h &= 1 \\
F &= 16.3527 \\
E &= 10000 \\
\nu &= 0.3
\end{aligned}
$$

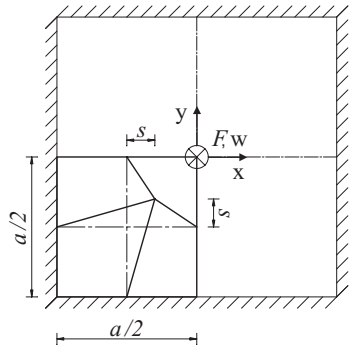

Figure 4: Clamped square plate subjected to a concentrated load

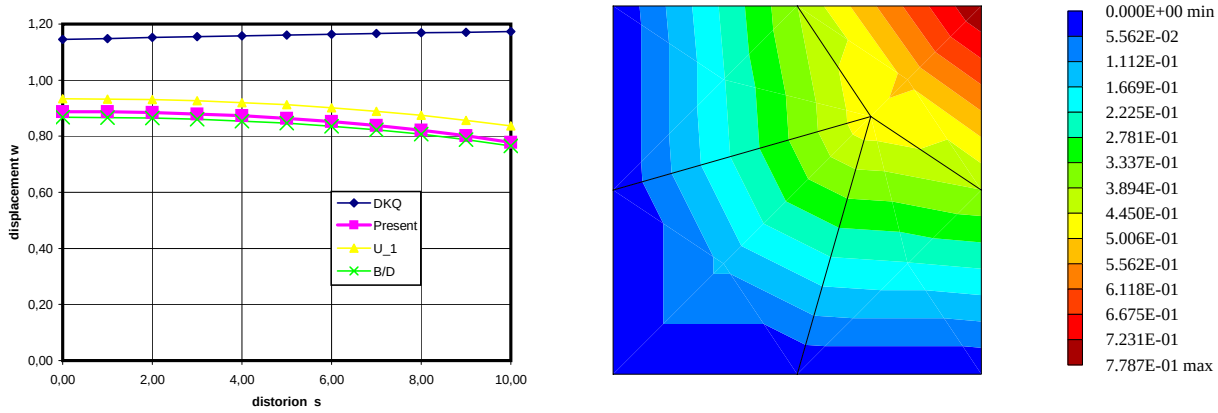

Figure 5: Influence of mesh–distorsion on center deflection and displacements for a mesh distorsion s=10

3.3 Corner supported square plate subjected to uniform load

A corner supported plate with edge length $2a$ subjected to uniform load is discussed. Considering symmetry the mesh consists of 8×8 elements for a quarter of the plate, see Fig. 6. The geometrical and material data are also given. An approximate ansatz according to [20] reads

$$w(x,y) = c_1 + c_2 x^2 + c_3 y^2 + c_4 x^4 + c_5 x^2 y^2 + c_6 y^4 \,, \tag{26}$$

where the origin of the co-ordinate system lies in the center of the plate. The boundary condition of vanishing bending moments at the edges can only be fulfilled in an integral sense. The other boundary conditions and the partial differential equation can be fulfilled exactly. The constants are determined and thus for $y = 0$ the approximate Kirchhoff solution reads

$$w(x, y=0) = \frac{qa^4}{2Eh^3}[11 - 6\nu - \nu^2 + (-5 + 4\nu + \nu^2)(\frac{x}{a})^2 + (1 + \frac{\nu}{2} - \frac{\nu^2}{2})(\frac{x}{a})^4] \,. \tag{27}$$

The deflections $w(x, y = 0)$ obtained with different elements are plotted in Fig. 7. The Belytschko/Tsay element [8] leads to hourglass modes for parameters $r_w < 0.02$, optimal

$a = 12$
$h = 0.375$
$q = 0.03125$
$E = 430000$
$\nu = 0.38$

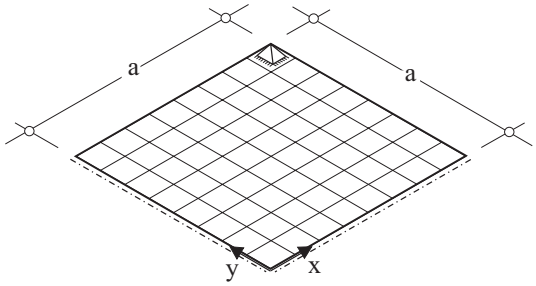

Figure 6: Corner supported plate

results for $0.02 \leq r_w \leq 0.05$ and locking for $r_w > 0.05$, see also [8]. The parameter $r_\beta = 0.02$ has been chosen constant in all cases. Furthermore the deformed mesh using the present element amplified by a factor 10 is depicted in Fig. 7. It can be seen that no hourglassing effects occur.

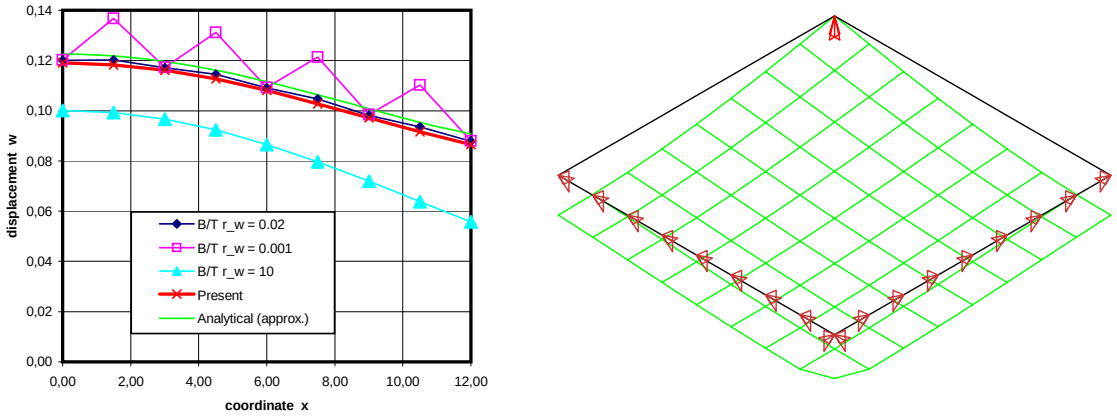

Figure 7: Deflection $w(x, y = 0)$, comparison of different elements and deformed mesh

For a convergence study of the center displacement the shear correction factor is increased for the present element and the Bathe/Dvorkin element to approximate the Kirchhoff solution. The results according to Table 1 show nearly the same convergence behaviour for all three compared elements against the same value, which differs from the approximate analytical solution.

	8*8	16*16	24*24	48*48	96*96	192*192
DKQ	0.11914	0.11960	0.11969	0.11974	0.11975	0.11976
B/D ($\kappa = 1000$)	0.11856	0.11946	0.11963	0.11973	0.11975	0.11976
Present ($\kappa = 1000$)	0.11862	0.11947	0.11963	0.11973	0.11975	0.11976
analytical (approx.)						0.12253

Table 1: Corner supported plate, convergence study

3.4 Concrete plate structure subjected to uniform load

A typical concrete plate structure of a building subjected to uniform load is presented in the final example, see Fig. 8. The plate of constant thickness $h = 0.25\ m$ is loaded with $q = -10\ kN/m^2$ and simply supported at the walls. A linear elastic material behaviour with $E = 3 \cdot 10^7\ kN/m^2$ and $\nu = 0.2$ is chosen. The plate is discretized with 3628 elements and 3790 nodes. The associated displacements w in cm are depicted in Fig. 8, where the minimum occurs around the hole. Similar results are obtained with the DKQ–element, [2]. Here, a comparison of CPU-time shows that in our implementation the DKQ-element needs about 52% more time than the present element for calculating the global stiffness matrix.

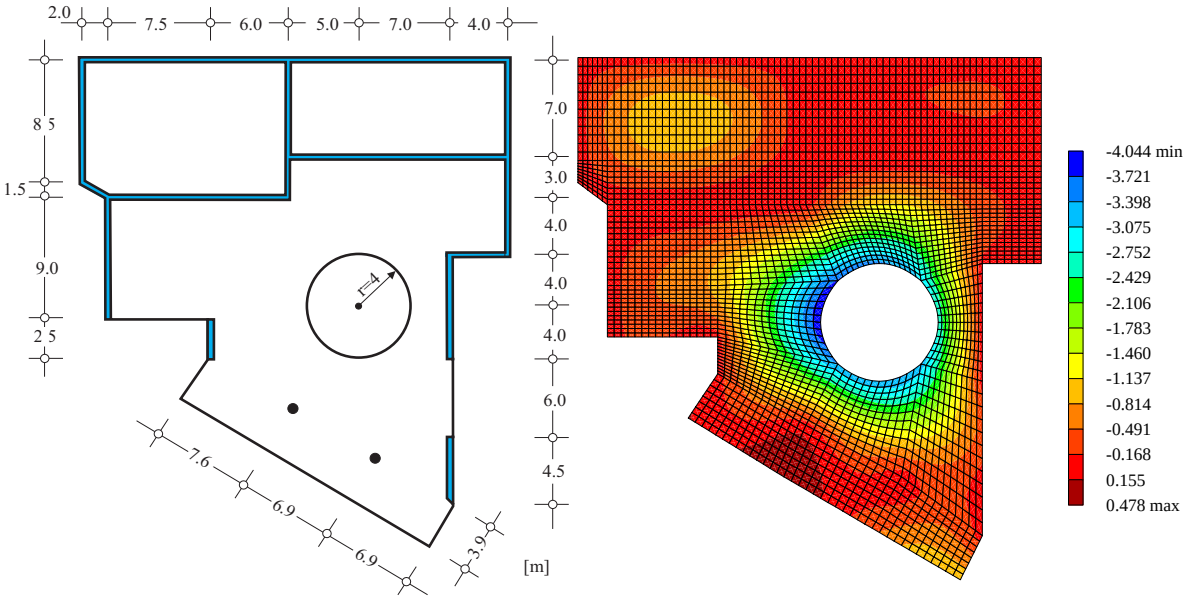

Figure 8: Concrete plate structure: system and displacement w in [cm]

4 CONCLUSIONS

The formulation of a quadrilateral plate element with three displacement degrees of freedom (transverse deflection, two rotations) at each node has been presented. The element possesses a correct rank, does not show shear locking and is applicable for the evaluation of displacements and stress resultants within the whole range of thin and thick plates. No parameters have to be adjusted to avoid shear locking or to prevent zero energy modes. The computed results are very satisfactory. The convergence behaviour for the displacements and stresses is slightly better than comparable quadrilateral assumed strain elements. However the essential advantage is the fast stiffness computation due to the analytically derived stiffness.

REFERENCES

[1] O.C. Zienkiewicz and R.L. Taylor. *The Finite Element Method*, Vol.1–3, 5. ed., Butterworth-Heinemann, Oxford, 2000.

[2] J. L. Batoz and M. B. Tahar. Evaluation of a New Quadrilateral Thin Plate Bending Element, *Int. J. Num. Meth. Engng.* **21**, 1655–1677, 1982.

[3] E. Reissner. The effect of transverse shear deformation on the bending of elastic plates, *J. Appl. Mech.* **12**, 69–76, 1945.

[4] R. D. Mindlin. Influence of rotatory inertia and shear flexural motions of isotropic elastic plates, *J. Appl. Mech.* **18**, 31–38, 1951.

[5] S. P. Timoshenko and S. Woinowsky–Krieger. *Theory of Plates and Shells*, McGraw–Hill 2^{nd}ed, 1970.

[6] O. C. Zienkiewicz, J. Too and R.L. Taylor. Reduced integration techniques in general analysis of plates and shells, *Int. J. Num. Meth. Engng.*, **3**, 275–290, 1971.

[7] T. R. J. Hughes, R. L. Taylor and W. Kanoknukulchai. A simple and efficient finite element for plate bending, *Int. J. Num. Meth. Engng.*, **11**, 1529–1543, 1977.

[8] T. Belytschko and S.-H. Tsay. A stabilization procedure for the quadrilateral plate element with one–point quadrature, *Int. J. Num. Meth. Engng.*, **19**, 405–419, 1983.

[9] T. Belytschko and W. Bachrach. Efficient implementation of quadrilaterals with high coarse–mesh accuracy, *Comp. Meth. Appl. Mech. Engng.*, **54**, 279–301, 1986.

[10] S. Reese and P. Wriggers. A stabilization technique to avoid hourglassing in finite elasticity, *Int. J. Num. Meth. Engng.*, **48**, 79–109, 2000.

[11] R. H. MacNeal. A simple quadrilateral shell element, *Comput. Struct.*, **8**, 175–183, 1978.

[12] T. J. R. Hughes and T. E. Tezduyar. Finite elements based upon Mindlin plate theory, with particular reference to the 4–node bilinear isoparametric element, *J. Appl. Mech.*, **48**, 587–595, 1981.

[13] R. H. MacNeal. Derivation of element stiffness matrices by assumed strain distribution, *Nuclear Engineering Design*, **70**, 3–12, 1982.

[14] E. Dvorkin and K.-J. Bathe. A Continuum Mechanics Based Four Node Shell Element for General Nonlinear Analysis, *Engineering Computations*, **1**, 77–88, 1984.

[15] K.-J. Bathe and E. Dvorkin. A 4–Node Plate Bending Element based on Mindlin/Reissner Theory and a Mixed Interpolation, *Int. J. Num. Meth. Engng.*, **21**, 367–383, 1985.

[16] E. Hinton and H. C. Huang. A family of quadrilateral Mindlin plate elements with substitute shear strain fields. *Comp. Struct.*, **23**, 409–431, 1986.

[17] T. H. H. Pian, D. Kang and C. Wang. Hybrid plate elements based on balanced stresses and displacements, *Finite Element Methods for Plate and Shell Structures*, Vol. 1, Pineridge Press, Swansea, 244–265, 1986.

[18] R. L. Taylor, J. C. Simo, O. C. Zienkiewicz and A. C. H. Chan. The patch test - A condition for assessing FEM convergence, *Int. J. Num. Meth. Engng.*, **22**, 39–62, 1986.

[19] T. H. H. Pian and K. Sumihara. Rational approach for assumed stress finite elements. *Int. J. Num. Meth. Eng.*, **20**, 1685-1695, 1984.

[20] S. L. Lee and P. Ballesteros. Uniformly loaded rectangular plate supported at corners, *Int. J. Mech. Sci.*, **2**, 206–211, 1960.